

The solution of (5) is then constructed as follows

$$Ge = \begin{cases} Je_{(L_2)}(h, \cosh u), & 0 \leq u < u_0 \\ fe_{(L_2)}(h, u_1, u), & u_0 < u \leq u_1. \end{cases} \quad (8)$$

However, equation (8) still does not satisfy the continuity condition at the point $u = u_0$. i.e.

$$G|_{u=u_0^-} = G|_{u=u_0^+} \quad (9a)$$

$$\frac{dG}{du}|_{u=u_0^-} - \frac{dG}{du}|_{u=u_0^+} = \delta(v - v_0). \quad (9b)$$

For condition (9a) to be satisfied, (8) requires a modification of the magnitude; thus

$$Ge = \begin{cases} Je_{(L_2)}(h, \cosh u) fe_{(L_2)}(h, u_1, u_0), & 0 \leq u < u_0 \\ fe_{(L_2)}(h, u_1, u) Je_{(L_2)}(h, \cosh u_0), & u_0 < u \leq u_1. \end{cases} \quad (10)$$

$$Ge(u, v|u_0, v_0) = \sum_{n=0}^{\infty} \frac{Je_n(h, \cosh u) fe_n(h, u_1, u_0) Se_n(h, \cos v) Se_n(h, \cos v_0)}{M_n^e(h) Je_n'(h, \cosh u_1)} \quad (17a)$$

In a similar manner, the odd Green's function is then

$$Go(u, v|u_0, v_0) = \sum_{n=1}^{\infty} \frac{Jo_n(h, \cosh u) fo_n(h, u_1, u_0) So_n(h, \cos v) So_n(h, \cos v_0)}{M_n^o(h) Jo_n'(h, \cosh u_1)} \quad (17b)$$

Applying condition (9b) to (10), we have

$$\frac{dG}{du}|_{u=u_0^-} - \frac{dG}{du}|_{u=u_0^+} = Je_{(L_2)}'(h, \cosh u_0) fe_{(L_2)}(h, u_1, u_0) - fe_{(L_2)}'(h, u_1, u_0) Je_{(L_2)}(h, \cosh u_0).$$

With some manipulation and the fact that $fe_{(L_2)}(h, u_0, u_0) = 1$ (i.e. the Wronskian $W(Je_n, Ye_n) = 1$), we arrive at

$$\frac{dG}{du}|_{u=u_0^-} - \frac{dG}{du}|_{u=u_0^+} = Je_{(L_2)}'(h, \cosh u_1) \quad (11)$$

Thus for condition (9b) to be satisfied, (10) has to be multiplied by $\delta(v - v_0)/Je_{(L_2)}'(h, \cosh u_1)$, hence we have

$$Ge = \begin{cases} \frac{Je_{(L_2)}(h, \cosh u) fe_{(L_2)}(h, u_1, u_0) \delta(v - v_0)}{Je_{(L_2)}'(h, \cosh u_1)}, & 0 \leq u \leq u_0 \leq u_1 \\ \frac{fe_{(L_2)}(h, u_1, u) Je_{(L_2)}(h, \cosh u_0) \delta(v - v_0)}{Je_{(L_2)}'(h, \cosh u_1)}, & 0 \leq u_0 \leq u \leq u_1. \end{cases} \quad (12)$$

Equation (12) is the complete even solution of (2b). However, this solution as it stands is impractical, as it involves a complicated function of the operator L_2 . To obtain a useful solution, further transformations are required. For these transformations, the eigenvalues and normalized eigenfunctions of the operator L_2 are needed. These are obtained by assuming L_1 is constant. This results in the homogeneous equation

$$\frac{d^2 V}{dv^2} + \left(L_1 - \frac{h^2}{2} \cos 2v \right) V = 0 \quad (13)$$

which is the circumferential Mathieu differential equation and has

the following eigenvalues and normalized eigenfunctions,

$$\lambda_n = n; Ve_n = \frac{Se_n(h, \cos v)}{[M_n^e(h)]^{1/2}} \quad (14)$$

Again only the even solutions are considered; the odd solutions have a similar format. Now as the functions are complete and orthonormal, we have by [2, p. 264]

$$\delta(v - v_0) = \sum_{n=0}^{\infty} \frac{Se_n(h, \cos v) Se_n(h, \cos v_0)}{M_n^e(h)} \quad (15)$$

also by [2, p. 259] for any continuous function $F(n)$, we have

$$F(L_2) \delta(v - v_0) = \sum_{n=0}^{\infty} F(n) \frac{Se_n(h, \cos v) Se_n(h, \cos v_0)}{M_n^e(h)}. \quad (16)$$

Using (16) to simplify (12), one has

where

$$fo_n(h, u_1, u_0) = Yo_n'(h, \cosh u_1) Jo_n(h, \cosh u_0) - Jo_n'(h, \cosh u_1) Yo_n(h, \cosh u_0);$$

the complete Green's function is then given by

$$G(u, v|u_0, v_0) = Ge(u, v|u_0, v_0) + Go(u, v|u_0, v_0). \quad (18)$$

Note that the above Green's function is for a unit impulse only, to obtain the Green's function for the patch one needs only to multiply equation (18) by $j\omega d$.

III. IMPEDANCE

The elements of the impedance matrix for a multiport elliptic disk are given by

$$Z_{ij} = \frac{1}{W_i W_j} \int_{W_i} \int_{W_j} G(s|s_0) ds ds_0 \quad (19)$$

For the elliptic patch, this reduces to

$$Z_{ij} = \frac{l^2}{W_i W_j} \int_{v_i - \Delta_i}^{v_i + \Delta_i} \int_{v_j - \Delta_j}^{v_j + \Delta_j} G(u_i, v|u_j, v_0) \cdot [\sinh^2 u_i + \sin^2 v]^{1/2} [\sinh^2 u_j + \sin^2 v_0]^{1/2} dv_0 dv \quad (20)$$

where

W_i = Width of Port,

$$\Delta_i \cong \sin^{-1} \left[\frac{W_i}{2l \sqrt{\sinh^2 u_i + \sin^2 v_i}} \right].$$

Substituting for Go from (17) and defining

$$ISe_n(h, v_i, \Delta_i, u_i) = \int_{v_i - \Delta_i}^{v_i + \Delta_i} Se_n(h, \cos v) \cdot [\sinh^2 u_i + \sin^2 v]^{1/2} dv \quad (21a)$$

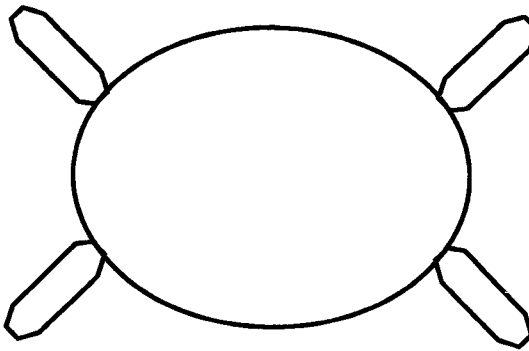
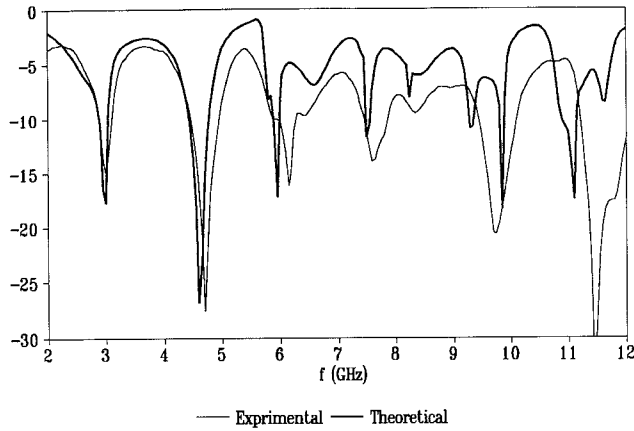


Fig. 2. Four port elliptic patch.

Fig. 3. Experiment and theoretical results for $|S_{11}|$.

$$ISo_n(h, v_i, \Delta_i, u_i) = \int_{v_i - \Delta_i}^{v_i + \Delta_i} So_n(h, \cos v) \cdot [\sinh^2 u_i + \sin^2 v]^{1/2} dv. \quad (21b)$$

$$Z_y^e = \frac{j\omega\mu dl^2}{W_i W_j} \sum_{n=1}^{\infty} \frac{Jo_n(h, \cosh u_i) ISo_n(h, v_i, \Delta_i, u_i) ISo_n(h, v_j, \Delta_j, u_j)}{M_n^e(h) Jo'_n(h, \cosh u_1)}. \quad (23b)$$

The above integrals can be evaluated using numerical integration.

The impedance elements are then given by

$$Z_y^e = \frac{j\omega\mu dl^2}{W_i W_j} \sum_{n=0}^{\infty} \frac{Je_n(h, \cosh u_i) fe_n(h, u_1, u_j) ISe_n(h, v_i, \Delta_i, u_i) ISe_n(h, v_j, \Delta_j, u_j)}{M_n^e(h) Je'_n(h, \cosh u_1)} \quad (22a)$$

$$Z_{ij}^o = \frac{j\omega\mu dl^2}{W_i W_j} \sum_{n=1}^{\infty} \frac{Jo_n(h, \cosh u_i) fo_n(h, u_1, u_j) ISo_n(h, v_i, \Delta_i, u_i) ISo_n(h, v_j, \Delta_j, u_j)}{M_n^o(h) Jo'_n(h, \cosh u_1)} \quad (22b)$$

$$0 \leq u \leq u_0 \leq u_1$$

where

$$fe_n(h, u_1, u_0) = Ye'_n(h, \cosh u_1) Je_n(h, \cosh u_0) - Je'_n(h, \cosh u_1) Ye_n(h, \cosh u_0)$$

$$fo_n(h, u_1, u_0) = Yo'_n(h, \cosh u_1) Jo_n(h, \cosh u_0) - Jo'_n(h, \cosh u_1) Yo_n(h, \cosh u_0).$$

For the special case when $u_j = u_1$, i.e. when the J th ports are at the periphery j using the Wronskian of Mathieu functions, the impedance matrix elements reduce to

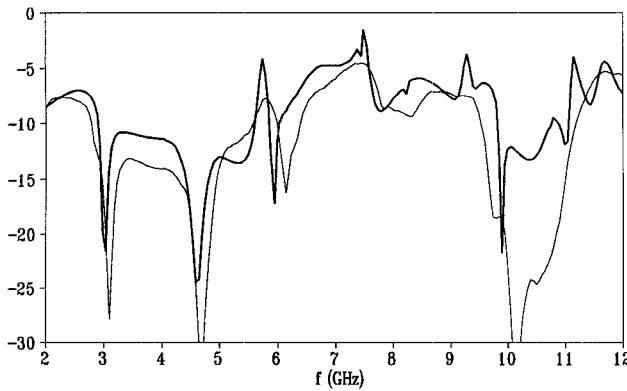
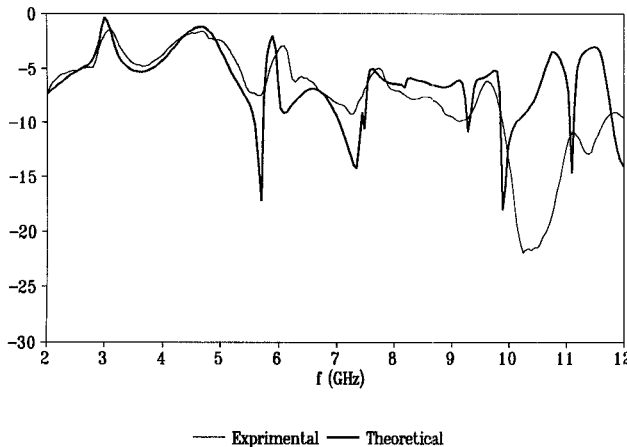
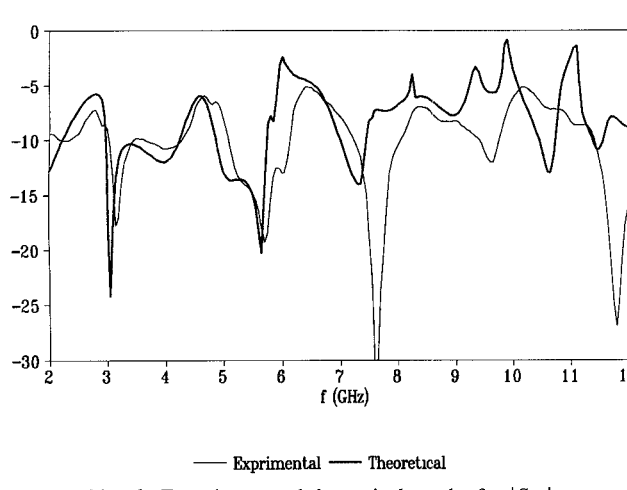
$$Z_y^e = \frac{j\omega\mu dl^2}{W_i W_j} \sum_{n=1}^{\infty} \frac{Je_n(h, \cosh u_i) ISe_n(h, v_i, \Delta_i, u_i) ISe_n(h, v_j, \Delta_j, u_1)}{M_n^e(h) Je'_n(h, \cosh u_1)} \quad (23a)$$

The matrix elements are then

$$Z_y = Z_y^e + Z_y^o \quad (24)$$

IV. EXPERIMENTAL AND THEORETICAL RESULTS

A four port elliptic was fabricated with dimensions of 4.6 cm major axis and 3.6 cm minor axis. The substrate was 1.524 mm thick, with $\epsilon_r = 2.5$. The ports were located at (30°, 150°, 210°, 330°) respectively, see Fig. 2, having width = 4.4 mm and impedance of 50 Ω. The experimental and theoretical responses of the patch are shown in Figs. 3-6. It should be pointed out that connector effects have not been accounted for, and the radiation losses have not been included in the calculation. However, the effective size and permittivity of the patch are used in the computation. Bearing this in mind, the agreement between theory and experiment

Fig. 4. Experiment and theoretical results for $|S_{12}|$.Fig. 5. Experiment and theoretical results for $|S_{13}|$.Fig. 6. Experiment and theoretical results for $|S_{14}|$.

is fairly good below 8 GHz, but understandably, diverges away gracefully above 8 GHz.

The effective permittivity used is given by

$$\epsilon_{\text{eff}} = \frac{\epsilon_r + 1}{2} + \frac{\epsilon_r - 1}{2} \left[1 + \frac{10d}{l(\cosh u_1 + \sinh u_1)} \right]^{-1/2}$$

where $u_1 = \tanh^{-1} (\text{Major}/\text{Minor})$.

The effective major and minor axis are calculated using

$$a_{\text{eff}} = a \left[1 + \frac{2d}{\pi a} \left\{ \ln \left(\frac{\pi a}{2d} \right) + 1.7726 \right\} \right]^{1/2}.$$

V. CONCLUSION

Elliptic cross-section devices have not been utilized much in the past, due to numerical difficulty and the resultant computational effort required to accurately predict the response. The Green's function for the elliptic patch derived in this paper reduces the computational effort considerably. High degree of convergence was achieved with about $n = 12$ modes.

APPENDIX FORMS OF MATHIEU FUNCTIONS

The definition followed in this paper are as given by Morse [1], with some modifications. There are several different series for evaluating Mathieu functions. The reader should be aware that some published series [1] and [3] are not convergent over the whole z -plane. It has been found during the course of the computation of Mathieu functions, that the following forms of Mathieu series are highly convergent.

First kind even circumferential Mathieu function

$$Se_{2n+p}(h, \cos v) = \sum_{m=0}^{\infty} A_{2m+p} \cos (2m + p)v. \quad (25)$$

First kind odd circumferential Mathieu function

$$So_{2n+p}(h, \cos v) = \sum_{m=0}^{\infty} B_{2m+p} \sin (2m + p)v. \quad (26)$$

First kind even radial Mathieu function

$$Je_{2n+p}(h, \cosh u) = \sqrt{\frac{\pi}{2}} \sum_{m=0}^{\infty} (-1)^{n-m} A_{2m+p} J_{2m+p}(h, \cosh u). \quad (27)$$

First kind odd radial Mathieu function

$$Jo_{2n+p}(h, \cosh u) = \sqrt{\frac{\pi}{2}} \tanh u \sum_{m=0}^{\infty} (-1)^{n-m} \cdot (2m + 1) B_{2m+p} J_{2m+p}(h, \cosh u). \quad (28)$$

Second kind even radial Mathieu function

$$Ye_{2n}(h, \cosh u)$$

$$= \frac{\sqrt{\frac{\pi}{2}}}{A_0} \sum_{m=0}^{\infty} (-1)^{n-m} A_{2m} Y_m \left(\frac{1}{2} h e^u \right) J_m \left(\frac{1}{2} h e^{-u} \right) \quad (29)$$

$$Ye_{2n+1}(h, \cosh u)$$

$$= \frac{\sqrt{\frac{\pi}{2}}}{A_1} \sum_{m=0}^{\infty} (-1)^{n-m} A_{2m} \left[Y_{m+1} \left(\frac{1}{2} h e^u \right) J_m \left(\frac{1}{2} h e^{-u} \right) + Y_m \left(\frac{1}{2} h e^u \right) J_{m+1} \left(\frac{1}{2} h e^{-u} \right) \right]. \quad (30)$$

Second kind odd radial Mathieu function

$$Yo_{2n+p}(h, \cosh u)$$

$$\begin{aligned} &= \frac{\sqrt{\frac{\pi}{2}}}{B_{2-p}} \sum_{m=0}^{\infty} (-1)^{n-m} B_{2m+p} \left[Y_{m+1} \left(\frac{1}{2} h e^u \right) J_{m-1+p} \right. \\ &\quad \left. \cdot \left(\frac{1}{2} h e^{-u} \right) - Y_{m-1+p} \left(\frac{1}{2} h e^u \right) J_{m+1} \left(\frac{1}{2} h e^{-u} \right) \right] \end{aligned} \quad (31)$$

Where $p \in \{0, 1\}$ and J_m , Y_m are the conventional Bessel functions.

The normalization constants are

$$\begin{aligned} M_{2n}^e(h) &= \int_0^{2\pi} [Se_{2n}(h, \cos v)]^2 dv \\ &= 2\pi \sum_{m=0}^{\infty} A_{2m}^2 / \sigma_m; \quad \sigma_m = \begin{cases} 1 & m = 0 \\ 2 & m \neq 0 \end{cases} \\ M_{2n+1}^e(h) &= \int_0^{2\pi} [Se_{2n+1}(h, \cos v)]^2 dv = \pi \sum_{m=0}^{\infty} A_{2m+1}^2 \\ M_{2n+p}^o(h) &= \int_0^{2\pi} [So_{2n+p}(h, \cos v)]^2 dv = \pi \sum_{m=1}^{\infty} B_{2m+p}^2. \end{aligned}$$

ACKNOWLEDGMENT

The support of the National Guard of Saudi Arabia is gratefully acknowledged. Also our thanks are due to Dr. D. Wait of NIST for supplying us with reference [4].

REFERENCES

- [1] P. M. Morse and H. Feshbach, *Methods of Theoretical Physics*. New York: McGraw-Hill, 1953.
- [2] G. F. Roach, *Greens Functions*. New York: Van Nostrand Reinhold, 1970.
- [3] N. W. McLachlan, *Theory and Applications of Mathieu Functions*. Oxford: Oxford University Press, 1947.
- [4] National Bureau of Standards, "Tables relating to Mathieu functions, characteristic values, and joining factors," *NBS 59*, reissue, with additions, New York: Columbia University Press, Aug. 13, 1967.
- [5] K. C. Gupta *et al.*, *Computer Aided Design of Microwave Circuits*. Dedham, MA: Artech House, 1981, p. 247.
- [6] D. A. Goldberg, L. Jackson, and R. A. Rimmer, "Modes of elliptical waveguides: a correction," *IEEE Trans. Microwave Theory Tech.*, vol. 38, pp. 1603-1608, Nov. 1990.
- [7] M. C. Bailey and M. D. Deshpande, "Analysis of elliptical and circular microstrip antennas using moment method," *IEEE Trans. Antennas Propagat.*, vol. AP-33, pp. 954-959, Sept. 1985.
- [8] A. K. Sharma and B. Bhat, "Spectral domain analysis of elliptic microstrip disk resonators," *IEEE Trans. Microwave Theory Tech.*, vol. MTT-28, pp. 573-576, June 1980.
- [9] T. M. Habashy, J. A. Kong, and W. C. Chew, "Resonance and radiation of the elliptic disk microstrip structure, Pt. I: formulation," *IEEE Trans. Antennas Propagat.*, vol. AP-35, pp. 877-885, Aug. 1987.
- [10] A. K. Bhattacharyya and L. Shafai, "Theoretical and experimental investigation of the elliptical annular ring antenna," *IEEE Trans. Antennas Propagat.*, vol. AP-36, pp. 1526-1530, Nov. 1988.
- [11] L. C. Shen, "The elliptical microstrip antenna with circular polarization," *IEEE Trans. Antennas Propagat.*, vol. AP-29, pp. 90-94, Jan. 1981.
- [12] F. A. Alhargan and S. R. Judah, "Reduced form of the Green's functions for disk and annular rings," *IEEE Trans. Microwave Theory Tech.*, vol. 39, no. 3, pp. 601-604, Mar. 1991.

On The Modal Expansion of Resonator Field in the Source Region

A. S. Omar, E. Jensen, and S. Lütgert

Abstract—Two field expansions for the electromagnetic field radiated by electric and magnetic currents in a cavity resonator are presented. The first utilizes the cavity resonant modes only, while the other utilizes, in addition, the irrotational modes. The first expansion is shown to be more suitable if the exciting currents have volume distributions. On the other hand, the second expansion is more suitable if the resonator contains surface or filamentary current distributions. Typical examples are given to demonstrate the convergence behavior of the two expansions near and within the source region.

INTRODUCTION

In a field-theoretical analysis of microwave tubes, e.g., klystrons, magnetrons, travelling wave tubes, gyrotrons, and orotron, one can divide the describing equations of the structure into two systems of equations. The first system expresses the electromagnetic field in terms of the exciting current(s). It is just Maxwell's equations with source terms. This system is linear if a small signal approximation is considered or if the nonlinear materials are replaced by polarization currents which can be added to the excitation ones. The second system describes the influence of the electromagnetic field on the motion of the electrons. It expresses then the exciting current(s) in terms of the excited field. This system is usually nonlinear except for the small signal analysis. The two systems must be solved simultaneously. They can be considered to represent a feedback system with a linear forward transmission and a nonlinear backward transmission. Well-established methods of control theory can consequently be applied to this feedback system in order to study the featuring characteristics like stability, starting and sustaining oscillation conditions, modulation, noise performance, etc.

The analysis of the linear system can be done in either time or frequency domain. In this paper, the analysis will be conducted in frequency domain. If time-domain information are needed, e.g., for the nonlinear system, an inverse Fourier transform must be made. Because the interaction between the electron beam and the electromagnetic wave in most of the microwave tubes takes place inside a cavity resonator, which may be either partially or completely shielded, the excited electromagnetic field can be expressed as expansions in terms of the empty cavity modes. These modes can be classified into divergence-free modes (which are the cavity resonant modes) and curl-free (or irrotational) modes.

The accuracy and convergence of these expansions is particularly important within the electron beam, i.e., in the source region, because accurate expressions for the electromagnetic field within the beam are necessary for the accurate solution of the nonlinear system (i.e., the electrons' equations of motion). It is the aim of this letter to study the different possible expansions along with their accuracy and convergence in the source region.

Manuscript received September 23, 1991; revised January 21, 1992. This work was supported by the Deutsche Forschungsgemeinschaft.

A. S. Omar is with Arbeitsbereich Hochfrequenztechnik, Technische Universität Hamburg-Harburg, Postfach 90 10 52, D-W-2100 Hamburg 90, Germany.

E. Jensen and S. Lütgert are with CERN, CH-1211 Geneva 23, Switzerland.

IEEE Log Number 9200865.